Metal-insulator transition and superconductivity in the spinel-type Cu(Ir1-xRhx)2S4 system

著者	MATSUMOTO Nobuhiro, ENDO Ryo, NAGATA Shoichi, FURUBAYASHI Takao, MATSUMOTO Takehiko

journal or publication title	Physical review. Third series. B, Condensed matter and materials physics
volume	60
number	8
page range	5258-5265
year	1999-08-15
URL	http://hdl.handle.net/10258/248

doi: info:doi/10.1103/PhysRevB.60.5258

Metal-insulator transition and superconductivity in the spinel-type $Cu(Ir_{1-x}Rh_x)_2S_4$ system

Nobuhiro Matsumoto, Ryo Endoh, and Shoichi Nagata*
Department of Materials Science and Engineering, Muroran Institute of Technology, 27-1 Mizumoto-cho, Muroran, Hokkaido, 050-8585 Japan

Takao Furubayashi and Takehiko Matsumoto
National Research Institute for Metals, 1-2-1 Sengen, Tsukuba, Ibaraki, 305-0047 Japan
(Received 20 November 1998)

The normal thiospinel $CuIr_2S_4$ exhibits a temperature-induced metal-insulator ($M-I$) transition around 226 K with structural transformation, showing hysteresis on heating and cooling. It has been verified that *d* electrons of Ir atom on the octahedral *B* sites have a significant role for the $M-I$ transition. On the other hand, $CuRh_2S_4$ is a superconductor with the transition temperature $T_c=4.70$ K, which is well understood on the basis of the BCS theory. It is important to investigate the effect on the $M-I$ transition by substitution of Rh for Ir. We have systematically studied structural transformation and electrical and magnetic properties of $Cu(Ir_{1-x}Rh_x)_2S_4$. The features of the $M-I$ transition change with Rh concentration *x*. A phase diagram of temperature versus *x* will be proposed for the $Cu(Ir_{1-x}Rh_x)_2S_4$ system. The sharp $M-I$ transition temperature varies drastically from 226 to 93 K with *x* from 0.00 to 0.17 and disappears around $x=0.20$. In a region of $0.00\leqslant x\leqslant 0.20$, the magnetic susceptibility begins decreasing at a constant onset temperature 226 K on cooling process and shows rather broad temperature variation, even though the metallic state is kept in the resistivity. The sharp $M-I$ transition can take place after the suppression of magnitude in the susceptibility has sufficiently developed far below 226 K. These experimental results are discussed with emphasis on the intrinsic difference between $Cu(Ir_{1-x}Rh_x)_2S_4$ and $CuIr_2(S_{1-x}Se_x)_4$ systems. Furthermore, we will mention the superconductivity for both systems of $Cu(Ir_{1-x}Rh_x)_2S_4$ with high-Rh concentration region and $Cu_{1-x}Ni_xRh_2S_4$. [S0163-1829(99)04331-3]

I. INTRODUCTION

Chalcogenide spinels, in particular copper-thiospinels including VIII-transition metals, have a large variety of physical properties.[1] Sulfides $CuCo_2S_4$, $CuRh_2S_4$, and $CuIr_2S_4$ have a cubic normal spinel structure. Cu ions occupy the *A* (tetrahedral) sites and VIII-transition-metal ions occupy the *B* (octahedral) sites. $CuCo_2S_4$ exhibits antiferromagnetism with the Néel temperature $T_N=17.5$ K.[2,3] An argument, whether coexistence of superconductivity and antiferromagnetism is possible or not in $CuCo_2S_4$, is in progress. $CuRh_2S_4$ becomes superconducting below the transition temperature $T_c=4.70$ K.[4–8] The characteristics of this type-II superconductor can be understood on the basis of the BCS theory.[7] In the normal state $CuRh_2S_4$ exhibits similar behavior to that of A15-type Nb_3Sn in the temperature dependence of electrical resistivity.[7,9] $CuIr_2S_4$ exhibits a temperature-induced metal-insulator ($M-I$) transition around 226 K with structural transformation, showing hysteresis on heating and cooling.[10–17] With decreasing temperature, a symmetry change occurs from cubic to tetragonal symmetry and a change from paramagnetism in metallic behavior to diamagnetism due to the atomic core orbital. A gap in the electronic density of states opens below the transition temperature of $CuIr_2S_4$. The majority of electrical carriers in the semiconductive (insulating) phase are holes, which is confirmed by Hall effect measurements used for hot-pressed sintering specimens.[18] The photoemission and Cu nuclear magnetic resonance measurements have verified that Cu ion has a monovalent state of Cu^+ in the low-temperature insulating state.[15,16] Therefore, the driving force to give rise to the cooperative Jahn-Teller distortion by Cu^{2+} ions disappears inherently from $CuIr_2S_4$. Consequently, the Jahn-Teller distortion effect is not a cause for the structural transformation in $CuIr_2S_4$.

Oda *et al.*[19,20] have performed theoretical band calculations for these cubic spinels. The Cu $3d$ orbitals are almost occupied by electrons, in other words Cu ions exist as Cu^+ rather than as Cu^{2+}, which supports our experimental results of $CuIr_2S_4$.[15,16] The hybridization between Co $3d\varepsilon$, Rh $4d\varepsilon$, Ir $5d\varepsilon$ orbitals and S $3p$ orbitals contributes mainly to the density of states (DOS) near the Fermi energy, $D(\epsilon_F)$. According to these calculations, the total DOS's at the Fermi level are 255, 130, and 83 states/(Ryd unit-cell), corresponding to $CuCo_2S_4$, $CuRh_2S_4$, and $CuIr_2S_4$, respectively. The total DOS decreases in the order of $CuCo_2S_4$, $CuRh_2S_4$, and $CuIr_2S_4$. The difference arises mainly from the band broadening due to the extent of wave functions of the *d* orbitals, which originates from the change of hybridization between *d* orbitals in the cations at *B* sites and $3p$ orbitals of sulfur. However, $CuRh_2S_4$ and $CuIr_2S_4$ have similar electronic structure and the same number of the occupied electrons in each outer *d* shell. Therefore, it is an important subject to investigate the effect on the $M-I$ transition by substitution of Rh for Ir. We expect that the most gradual variations of the $M-I$ transition can be observed by gentle chemical modification without any change of number of *d* electron in the outer shell. The clarification of mechanism of the $M-I$ transition may germinate from these variations.

We have successfully synthesized the specimens of $Cu(Ir_{1-x}Rh_x)_2S_4$. We have carried out a systematic experimental study of structural, electrical and magnetic properties of $Cu(Ir_{1-x}Rh_x)_2S_4$, in order to study the substitution effect

on the $M-I$ transition and on the superconductivity. The variation of Rh concentration x leads to a systematic change of the magnetic and electrical features. In particular, more characteristic changes have been observed in Ir-rich concentration region $0.00 \leqslant x \leqslant 0.20$. A phase diagram between temperature T and Rh concentration x has been determined experimentally for the system of $Cu(Ir_{1-x}Rh_x)_2S_4$. Recently, we have made a systematic investigation of $CuIr_2(S_{1-x}Se_x)_4$ system, where many interesting features have been found.[12,21–24] The inherent difference in the experimental results between $Cu(Ir_{1-x}Rh_x)_2S_4$ and $CuIr_2(S_{1-x}Se_x)_4$ system will be discussed. The superconductivity in $Cu(Ir_{1-x}Rh_x)_2S_4$ and $Cu_{1-x}Ni_xRh_2S_4$ will be also mentioned.

II. EXPERIMENTAL METHODS

The polycrystalline specimens were prepared by a direct solid-state reaction. Mixtures of high-purity fine powders of Cu(purity 99.99%), Ir(99.9%), Rh(99.99%), S(99.999%) with nominal stoichiometry were heated in sealed quartz tubes to 1123 K and kept at this temperature for 10 days. The resultant powder specimens were reground and pressed into rectangular bars at the pressure of 0.2 GPa at room temperature and then were heated to 1123–1273 K for 48 h. In high-Rh concentration $0.60 \leqslant x \leqslant 1.00$, since it was harder to prepare the high-purity and high-density sintering specimen, they were obtained by repeating this process for several times.

The identification of the crystal structure and the determination of the lattice constants were carried out by powder x-ray diffraction method using Cu Kα radiation from room temperature to 10 K. Low-temperature x-ray experiments down to 10 K were attained by a closed-cycle helium refrigerator.

The resistivity ρ of sintered specimens with dimensions of about $1.8 \times 1.8 \times 10$ mm^3 was measured by a standard dc four-probe method in the temperature range of 4.2 K to room temperature. Silver paste was used to form electrodes. The dc magnetic susceptibility χ of powder specimens solidified with cyanoacrylate adhesive was measured with a Quantum Design superconducting quantum interference device magnetometer in the range of $5 \leqslant T \leqslant 300$ K at intervals of 5 K in an applied magnetic field of 10 kOe. The weight ratio of adhesive to specimen was approximately 1:3, and the background contribution due to the adhesives was subtracted from the experimental values. For the observation of the Meissner effect in high-Rh-concentration region, zero-field cooling (ZFC) susceptibility was also measured by applying a magnetic field of 10 Oe above 2.0 K after cooling down to 2.0 K in the absence of field. Demagnetizing-field corrections were made for samples, assuming completely homogeneous sintering in the whole specimen with sphere shape.

III. RESULTS AND DISCUSSION

A. Metal-insulator transition in $Cu(Ir_{1-x}Rh_x)_2S_4$

Powder x-ray diffraction patterns at room temperature confirm that $Cu(Ir_{1-x}Rh_x)_2S_4$ has the normal-spinel type structure in all Rh-concentration range, although small impurities existed in high-Rh-concentration region. The lattice constant a is proportional to x at room temperature and varies from 9.85 Å for $x=0.00$ to 9.79 Å for $x=1.00$.

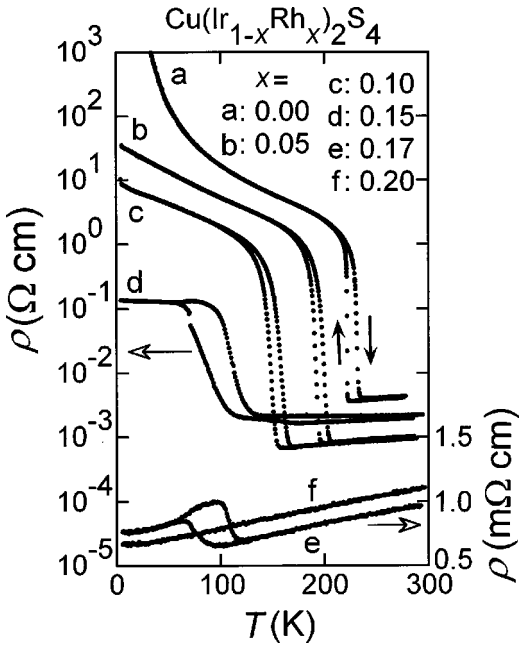

FIG. 1. Electrical resistivity ρ of sintered specimens $Cu(Ir_{1-x}Rh_x)_2S_4$ as a function of temperature T for the concentration range $0.00 \leqslant x \leqslant 0.20$. The left-hand side of the vertical axis has the logarithm scale for $0.00 \leqslant x \leqslant 0.15$, and the right of the linear scale for $x=0.17$ and 0.20.

Figure 1 shows the temperature dependence of electrical resistivity in the Ir-rich region $0.00 \leqslant x \leqslant 0.20$. The conductivity of $CuIr_2S_4$, $x=0.00$, abruptly drops by nearly three orders of magnitude around 226 K with hysteresis on heating and cooling. $CuIr_2S_4$ of the insulating state exhibits a thermally activated conductivity obeying the Arrhenius equation and has the activation energy of $q=4.7\times10^{-2}$ eV in the temperature range 140–200 K.[10,12,13] With increasing Rh concentration x, the $M-I$ transition temperature T_{M-I} decreases systematically and the height of the jump around T_{M-I} becomes smaller. The temperature dependence below T_{M-I} changes gradually from the semiconductive behavior to metallic one. Above $x=0.20$, simple metallic behavior is observed without the sharp jump in the resistivity.

Figure 2 shows the temperature dependence of magnetic susceptibility for the Ir concentration-rich region $0.00 \leqslant x \leqslant 0.20$. The value of χ indicates the magnetization M divided by the applied magnetic field H. Measurements were carried out on warming and cooling at a constant applied magnetic field of 10 kOe. The magnetic susceptibility of $CuIr_2S_4$ exhibits a sharp jump around $T_{M\text{-}I}=226$ K with temperature hysteresis. The high-temperature cubic phase shows the Pauli paramagnetism and the low-temperature phase indicates nonmagnetism except the small amount of the diamagnetism. The diamagnetic susceptibility is due to atomic cores and is estimated to be an order of 10^{-4} emu mol^{-1} for $Cu(Ir_{1-x}Rh_x)_2S_4$ by using the Pascal additive law,[25] and this order is reasonable one.

With increasing Rh-concentration x, the decrease of susceptibility seems to occur in more broader temperature region below 226 K. It should be noted on cooling process that onset temperature indicating of the susceptibility decrease is

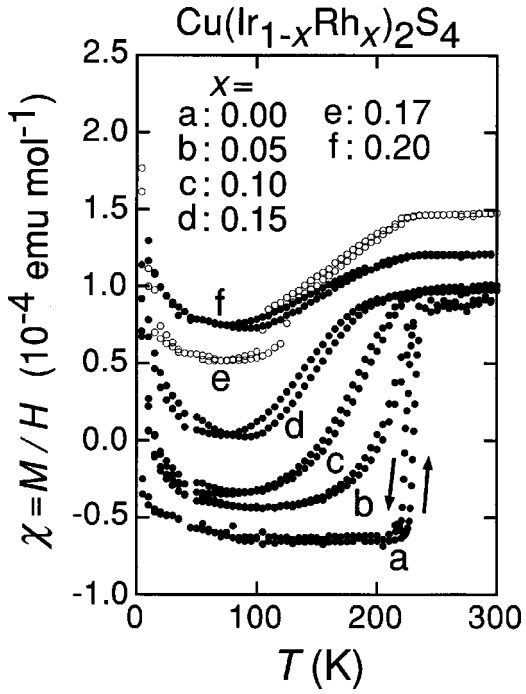

FIG. 2. Magnetic susceptibility χ versus temperature for powder specimens of $Cu(Ir_{1-x}Rh_x)_2S_4$ for the concentration range $0.00 \leqslant x \leqslant 0.20$.

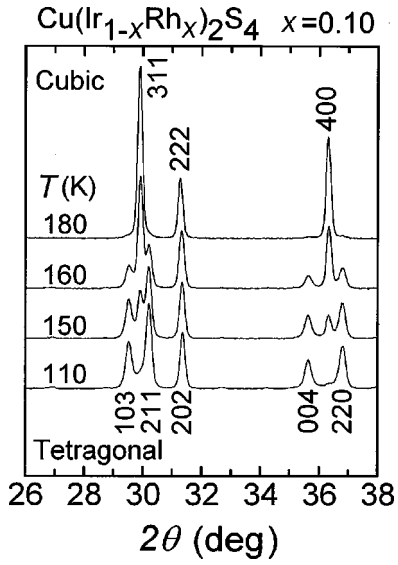

FIG. 3. Powder x-ray diffraction pattern at various temperatures for $x=0.10$ upon cooling.

independent of x, namely the onset temperature is kept around 226 K for $x \leqslant 0.20$. On cooling, the decrease of susceptibility has sufficiently developed in the metallic state far below 226 K, subsequently the sample enables to give rise to a cooperative crystal transformation, accompanying the sharp jump of the resistivity. If the positive temperature dependence of the susceptibility with $d\chi/dT \geqslant 0$ is intrinsic property in the metallic state, we may expect that the Fermi energy is situated in a region of the energy band with high DOS and there is a sharp peak of DOS just above the Fermi energy. Experimentally, the $T_{M\text{-}I}$ does not correspond to the onset temperature of the decrease in the susceptibility. Above 226 K, the susceptibility is nearly temperature independent and the value at room temperature goes up with x in the region of $0.00 \leqslant x \leqslant 0.20$.

All the samples of $Cu(Ir_{1-x}Rh_x)_2S_4$ have susceptibility increasing below about 50 K, where the value of the effective magnetic moment is estimated to be less than 0.15 μ_B per molecule from the value of the Curie constant, assuming the existence of localized moments. This value is much less than the spin-only moment 1.73 μ_B expected for $S=1/2$. There is no indication of any systematic variation of the effective moment with the value of x. This increase in the susceptibility at low temperatures may be due to the existence of the localized spins at impurity site or at other kind of lattice imperfection. Then, there seems to be no intrinsic localized magnetic moment in this system. Consequently, the substitution of Rh for Ir is unable to change or to break the magnetic state of $Cu(Ir_{1-x}Rh_x)_2S_4$, that is, the intrinsic localized moment is absent in the insulating phase.

Figure 3 shows the powder x-ray diffraction patterns of the sample $x=0.10$ at various temperatures near T_{M-I}. The crystal transformation is observed from cubic to tetragonal symmetry with decreasing temperature. At 180 K, the diffraction peaks can be indexed on the cubic symmetry with the space group $Fd3m$. At 160 and 150 K, the clear coexistence of the cubic and tetragonal symmetry can be seen, where two peaks from the cubic symmetry and three from the tetragonal are overlapped in the region of diffraction angle $29 \leqslant 2\theta \leqslant 32°$. One peak arisen from the cubic and two from the tetragonal overlap in $35 \leqslant 2\theta \leqslant 37°$. The diffraction peaks at 110 K are indexed on the tetragonal symmetry with the space group $I4_1/amd$ (Ref. 11). The temperature of crystal transformation corresponds fairly well to the midpoint of the abrupt increase in the resistivity.

In the higher concentration of $x=0.15$, both peaks from the cubic and tetragonal phases are observed below 170 K as shown in Fig. 4. Even at the lowest temperature of 10 K in our measurements, the coexistence can be observed. It is noted that the mixing ratio of the tetra to cubic phases is fixed below around 80 K, whereas the intensity of the tetragonal phase grows with decreasing temperature above 80 K. The similar behavior has been also found for the samples of $x=0.17$ and $x=0.20$, exhibiting the lower temperatures where the mixing ratio of the tetra to cubic phases is fixed.

Figure 5 shows the concentration dependence of diffraction patterns over a range of $0.00 \leqslant x \leqslant 1.00$ at the constant temperature of 10 K. Specimens of $x=0.00$ and 0.10 have tetragonal structure at 10 K. In the concentration range of $0.15 \leqslant x \leqslant 0.20$, there are both tetragonal and cubic phases. The specimens of $x=0.50$ and $x=1.00$ have only cubic phase. It is important to detect the feature of the coexistence of the cubic and tetragonal phases and to evaluate the volume of the each phase. We have never tried to detect with the electron microscope at low temperature because of the hard situation to accomplish these experiments. We have found only the particle size distribution of the order of 0.1 to 1 μm for the powder specimen of $x=0.15$ with a scanning electron microscope at room temperature.

Nevertheless, we conjecture that the coexistence occurs not in the macroscopic scale but in rather microscopic region and the each phase mixes homogeneously. This conjecture is indirectly supported by the macroscopic results that the tem-

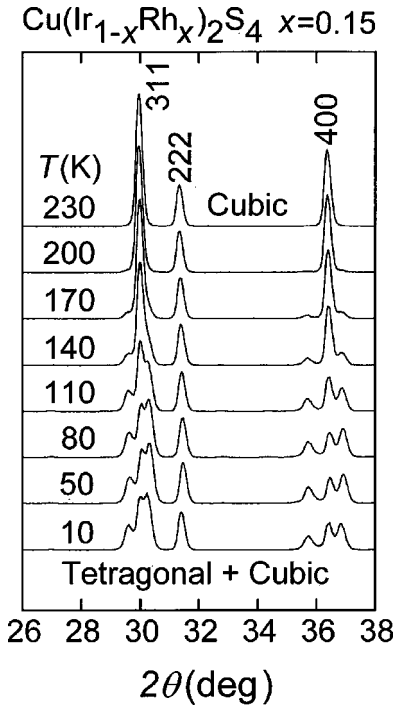

FIG. 4. Powder x-ray diffraction pattern at various temperatures for $x=0.15$ upon cooling.

perature dependences of the resistivity and magnetic susceptibility vary not irregularly but fairly smoothly over a wide-concentration region.

Figure 6 shows the diffraction patterns at 10 K in the range of $23\leqslant 2\theta\leqslant 29°$. Triangular marks indicate the weak peaks that are not observed at high temperatures but are detected only below the T_{M-I} for $0.00\leqslant x\leqslant 0.17$. These extremely small peaks cannot be explained by assuming the tetragonal symmetry with $I4_1/amd$ (Ref. 11). The intensity of these lines becomes weaker with increasing x. There is no

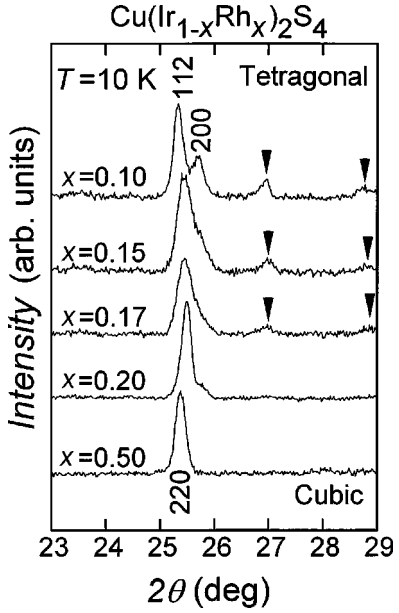

FIG. 6. Powder x-ray diffraction pattern of $Cu(Ir_{1-x}Rh_x)_2S_4$ at 10 K in the angle range of $23\leqslant 2\theta\leqslant 29°$. The triangles indicate the weak peaks originated presumably from the superstructure.

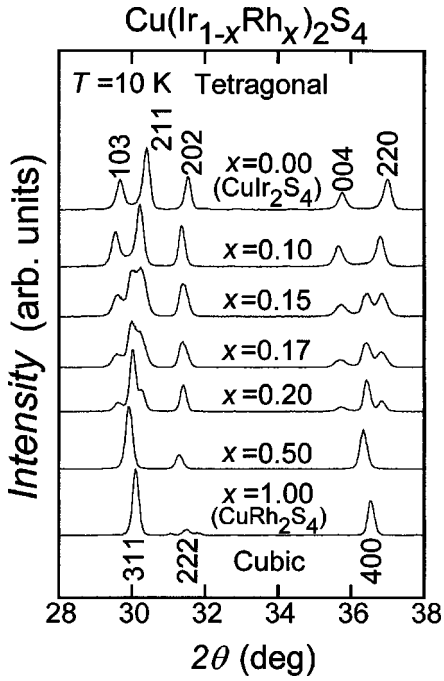

FIG. 5. Powder x-ray diffraction pattern of $Cu(Ir_{1-x}Rh_x)_2S_4$ at 10 K in the angle range of $28\leqslant 2\theta\leqslant 38°$.

weak line above $x=0.20$ whose specimen has no anomalous behavior on the temperature dependence of resistivity. Some periodic modulation or small atomic displacement with long period could cause these weak satellite peaks in x-ray patterns and may play an important role in the $M-I$ transition of $CuIr_2S_4$.

In the previous paper,[21] we have studied the substitution effect of Se at S sites, $CuIr_2(S_{1-x}Se_x)_4$. The selenospinel $CuIr_2Se_4$ exhibits pressure-induced metal-insulator transition,[26,27] while under the ambient pressure it remains metallic down to 0.5 K and its crystal structure holds cubic symmetry at 10 K.[12] In $CuIr_2(S_{1-x}Se_x)_4$, the $M-I$ transition temperature T_{M-I}, the structural transformation temperature, and the onset temperature of susceptibility decrease are almost the same for each Se concentration x. All the these sharp jumps with the hysteresis in the temperature dependence occur at the same temperature in $0.00\leqslant x\leqslant 0.15$ of $CuIr_2(S_{1-x}Se_x)_4$. The remarkable difference between $Cu(Ir_{1-x}Rh_x)_2S_4$ and $CuIr_2(S_{1-x}Se_x)_4$ systems could be significant to clarify the origin and the mechanism of the $M-I$ transition.

B. Superconductivity in $Cu(Ir_{1-x}Rh_x)_2S_4$

Figure 7 shows the susceptibility of $0.80\leqslant x\leqslant 1.00$ in an applied magnetic field of 10 Oe under the condition of ZFC, after demagnetizing-field corrections assuming that each particle in the specimen is sphere. The diamagnetic onset temperature shifts to lower temperature with increasing Ir concentration. The Ir substitution gives rise to a considerable broadening of the transition and the diamagnetic indication becomes weaker.

Figure 8 shows the magnetic susceptibility of specimens for $0.30\leqslant x\leqslant 1.00$ in the temperature range of 5 to 300 K in a field of 10 kOe. In this concentration range, the magnetic susceptibility exhibits no hysteresis loop on heating and

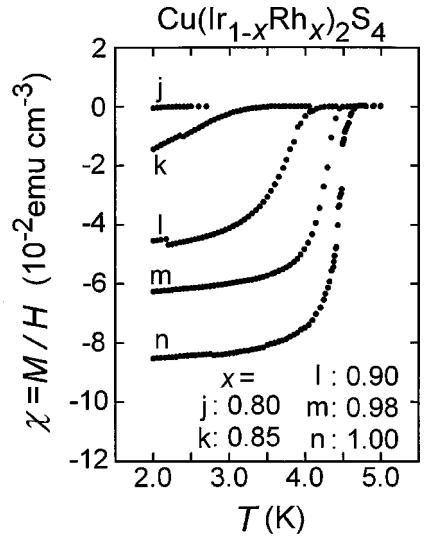

FIG. 7. Zero-field cooled diamagnetic susceptibility of $Cu(Ir_{1-x}Rh_x)_2S_4$ for the concentration range over $0.80 \leqslant x \leqslant 1.00$. The magnetic field of 10 Oe is applied in measuring.

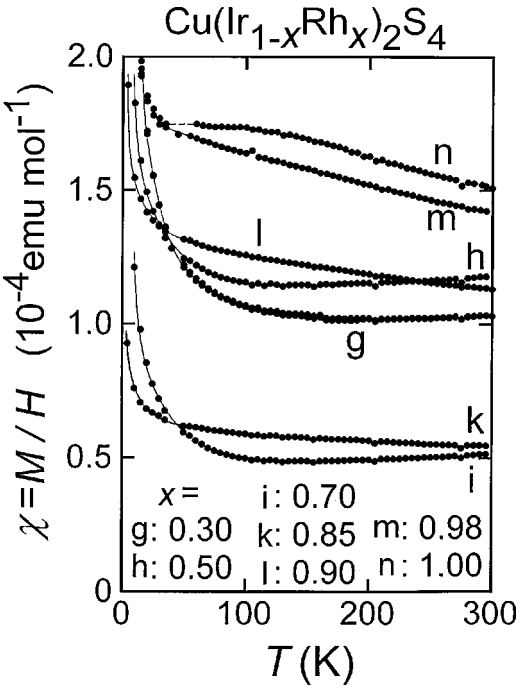

FIG. 8. Magnetic susceptibility of powder specimens $Cu(Ir_{1-x}Rh_x)_2S_4$ for the concentration range $0.30 \leqslant x \leqslant 1.00$. The applied magnetic field is 10 kOe.

cooling. The temperature derivative $d\chi/dT$ is slightly positive in higher temperature region than about 150 K for $0.30 \leqslant x \leqslant 0.70$. The $d\chi/dT$ is negative for $0.80 \leqslant x \leqslant 1.00$, where the superconducting state arises at low temperatures. The large increase in the susceptibility at low temperatures is caused mainly by extrinsic paramagnetic impurities that come from the defect with magnetic state, which is in the same situation of Fig. 2. No intrinsic localized moment has been observed in $0.30 \leqslant x \leqslant 1.00$. The magnitude of the susceptibility at room temperature seems to oscillate slowly with increasing x: increases for $0.00 \leqslant x \leqslant 0.50$, decreases for $0.50 \leqslant x \leqslant 0.70$, and increases again for $0.70 \leqslant x \leqslant 1.00$. The interpretation of this oscillation of susceptibility is complicated problem because not only the Pauli paramagnetism reflecting the $D(\epsilon_F)$ but also the Van Vleck temperature-independent paramagnetism originating from Ir and Rh atoms are superposed.

Figure 9 shows the temperature dependence of electrical resistivity in the range of $0.20 \leqslant x \leqslant 1.00$. The superconducting transition temperatures defined as midpoint are 4.70 and 4.68 K for $x = 1.00$ and 0.98, which correspond to the onset temperature of the susceptibility, respectively. No transition has been found above 4.2 K for $x = 0.90$. The resistivity of $CuRh_2S_4$, $x = 1.00$, rises rapidly up to about 100 K and then approaches gradually to a linear variation with a smaller slope that is similar behavior to that of A15-type Nb_3Sn.[7,9] On increasing Ir content in $0.90 \leqslant x \leqslant 1.00$, the value of the resistivity at room temperature becomes smaller, and the temperature dependence of resistivity becomes more straight. As can be seen in Fig. 9, the resistivity shows extremely small difference between $x = 0.20$ and 0.90. According to the BCS theory, the transition temperature T_c can be expressed as: $T_c \propto \Theta e^{-1/UD(\epsilon_F)}$ where Θ is the Debye temperature, and U is the strength of the electron-lattice interaction. The magnitude of resistivity at room temperature is a rough measure of the electron-lattice interaction. Suppose the value of Θ is unchanged, then T_c is evaluated in terms of U and $D(\epsilon_F)$. Both of the $D(\epsilon_F)$ and U decrease with increasing Ir concentration in $Cu(Ir_{1-x}Rh_x)_2S_4$.

A Nickel-included thiospinel $NiRh_2S_4$ exhibits simple metallic conduction and the Pauli paramagnetism with no anomaly.[28,29] In $Cu_{1-x}Ni_xRh_2S_4$,[30] the substitution system of Ni at Cu sites of $CuRh_2S_4$, T_c decreases rapidly with Ni concentration x and exhibits no superconducting transition above 2.0 K in $x \geqslant 0.10$. In the normal state, the temperature dependence of the resistivity in $Cu_{1-x}Ni_xRh_2S_4$ has also strongly influenced by increasing Ni concentration x, as well as $Cu(Ir_{1-x}Rh_x)_2S_4$. $D(\epsilon_F)$ increases with Ni concentration x, while the value of U decreases. The effect of the decreasing in U overcomes the increasing of $D(\epsilon_F)$, consequently T_c drops with increasing Ni concentration x. A Rh-contained selenospinel $CuRh_2Se_4$ is also a type-II superconductor of $T_c = 3.48$ K (Refs. 7 and 31) and the superconductivity can be understood on the basis of the BCS theory as well as $CuRh_2S_4$. Riedel *et al.*[32] have synthesized $CuRh_2(S_{1-x}Se_x)_4$ but the measurements of detailed physical properties have not been made.

C. Phase diagram

Figure 10 shows a phase diagram for T versus x, which simplifies the rather complicated structural and electrical characteristics in the system $Cu(Ir_{1-x}Rh_x)_2S_4$. In the left-hand side of this diagram, the cubic structure phase area at high temperatures is separated into the tetragonal one at low temperatures by the shaded area. This shaded area is the intermediate region where the cubic and tetragonal phases coexist, and expands progressively with the value of x. For example, in the sample of $x = 0.15$, this coexistence is clearly detected at 10 K. If the specimen were single crystal with high purity, this intermediate region might be shrunk or disappear. Since the pure material has a definite certain transition temperature, it is strange for the transformation temperature to spread. As one possible explanation, we attribute this

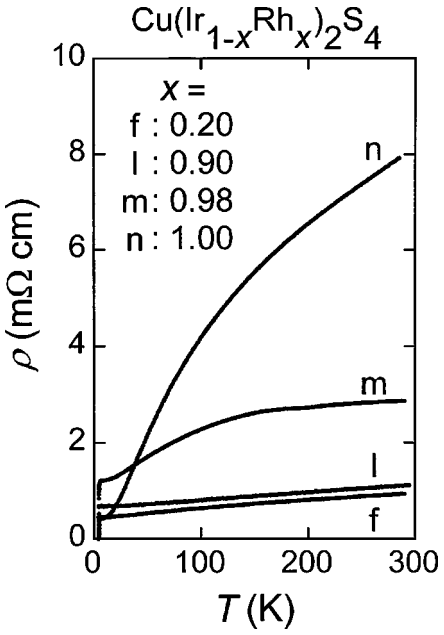

FIG. 9. Electrical resistivity of sintered specimens $Cu(Ir_{1-x}Rh_x)_2S_4$ as a function of temperature for the concentration range $0.20 \leqslant x \leqslant 1.00$. Note that only samples m and n exhibit resistivity decreases associated with the superconducting transition above 4.2 K.

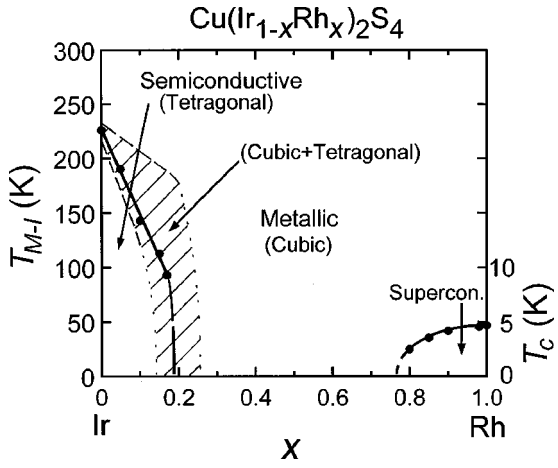

FIG. 10. Phase diagram of $Cu(Ir_{1-x}Rh_x)_2S_4$ for temperature versus concentration x. In the left-hand side, the solid circles indicates the $M-I$ transition temperature T_{M-I}. The shaded area indicates that the cubic and tetragonal phases coexist. In the right, the circles show the superconducting transition temperature T_c.

coexistence to the inhomogeneity of the concentration x in the specimen. In one specimen, the crystal transformation in lower concentration regions occurs at higher temperature than in higher concentration regions.

Another interpretation arises from the particle-size dependence of transition temperature under the influence of surface energy. Therefore, each particle or grain may have different transformation temperature. This particle size may have also strong influence on the spread of the coexistence region. The nucleation of the stable tetragonal phase in the matrix of the cubic phase depends delicately on the concentration x and the size of particles or grains. The shaded region, in particular around $0.15 \leqslant x \leqslant 0.20$, is under a complicated competing situation.

Solid circles for $x \leqslant 0.17$ show the abrupt $M-I$ transition temperature T_{M-I} in the resistivity. This T_{M-I} decreases linearly with x. Around $x=0.12$, the temperature dependence below T_{M-I} varies from the semiconductive to metallic behavior. The $M-I$ transition is seen in the region of $0.00 \leqslant x \leqslant 0.10$. The metal-metal transition occurs in $0.15 \leqslant x \leqslant 0.17$. The simple metallic conductivity is observed in $0.20 \leqslant x \leqslant 0.80$. The cubic symmetry has been verified at 10 K for the samples of $x=0.50$ and 1.00. It is fascinating that both of the temperature- and concentration-induced $M-I$ transitions are seen in the system of $Cu(Ir_{1-x}Rh_x)_2S_4$.

In the right-hand side in Fig. 10, solid circles represent the superconducting transition temperature T_c, which decreases with increasing Ir concentration. The linear metallic conductivity in the normal state changes into *S*-shape metallic conductivity with increasing Rh concentration x. The temperature coefficient of susceptibility above 150 K also changes from positive to negative around $x=0.80$ with increasing x.

D. Some other remarks

The detailed structure analysis is critically important to clarify and to discuss the mechanism for the $M-I$ transition. We have observed the x-ray superstructure pattern with very small intensity in the insulating phase. The appearance of this x-ray superstructure peaks may relate directly to the possibility of the charge disproportionation of Ir ions suggested by Mössbauer data[21] and also the sharp superstructure reflections appear in the electron diffraction pattern in addition to the basic Bragg diffraction spots.[33] Unfortunately, we are not able to analyze these results because of the scattering data from sample to sample at the present time. We are planning to provide a detailed structure analysis and to publish somewhere after a step of obtaining single crystals. We are now in progress to grow the single crystals of $CuIr_2S_4$.

There are some compounds which exhibit charge disproportionation, for example, $Ba_{1-x}K_xBiO_3$,[34] Fe_3O_4,[35] and $La_{1-x}Sr_xFeO_3$.[36] The relationship between crystal symmetry and charge disproportionation has been discussed in detail for single crystals of these compounds. In the present study using polycrystals of sulfides, no knowledge of the anisotropy in the physical properties is currently available. The experimental results include inevitably serious influence due to the sulfur deficiency and other chemical inhomogeneity in the samples. Furthermore, the sulfides have stronger covalent bonding and rather higher conductivity than oxides. Then, it is hard to compare directly the experimental results with these of oxides, which can be discussed on the basis of simplified model of ionic picture.

The experimental facts for the $M-I$ transition indicate the similar behavior in the intermediate doping regime for $Cu(Ir_{1-x}Rh_x)_2S_4$ and $CuIr_2(S_{1-x}Se_x)_4$ systems, whereas Rh substitution for Ir and Se substituion for S have opposite effects on unit cell size. It is stressed here that the change of the unit cell size is much larger in the system of the substitution of Se for S than that of Rh for Ir because of the big difference in the ionic radius between cation and anion. The substitution of Se for S influences strongly on the local structure and symmetry, that is, the symmetry of IrS_6 octahedra is completely distorted by substituting Se for S. On the other hand, even though the magnitude in the change of unit cell size of Rh substitution is much less than that of Se substitution, the alignment of IrS_6 octahedra along the direction cor-

responding to ⟨110⟩ of the cubic spinel structure could be disturbed and buckled by introducing the Rh atom in the insulating phase. The magnetic and electrical properties are strongly affected by introducing the local structure deviation from the pure spinel structure. It seems to be reasonable to expect the similar behavior of the variation of the $M-I$ transition for the intermediate doping regime for both systems. The oversimplified interpretation for the similar tendency of the changes in the electrical and magnetic properties, when the unit-cell size expands or contracts by these substitutions, should be excluded.

IV. SUMMARY

A phase diagram of $Cu(Ir_{1-x}Rh_x)_2S_4$ has been determined by systematic measurements of powder x-ray diffraction, electrical resistivity and magnetic susceptibility. Even if a small amount of Rh atoms is substituted for Ir, the characteristics of structural and physical properties are strongly influenced by this chemical modification. In an Ir-rich concentration region, the partial substitution lowers metal-insulator transition linearly and makes the electrical resistivity more metallic. The onset temperature of decreasing in the susceptibility is held to be constant of 226 K, even though abrupt $M-I$ jump in the resistivity changes largely with the value of x. This onset temperature 226 K is the exactly same temperature of the T_{M-I} of $CuIr_2S_4$. It is our hope that the results of present paper will help in clarifying the mechanism of the $M-I$ transition in $CuIr_2S_4$.

ACKNOWLEDGMENTS

The authors would like to thank Dr. I. Shimono (Hokkaido Industrial Technology Center, Hakodate) for energy dispersive x-ray spectroscopy (EDX) analysis and the SEM measurement. The authors are grateful to Dr. J. Tang (National Research Institute for Metals, Tsukuba) for her Hall effect measurements, and Mr. S. Yasuzuka (Hokkaido University, Sapporo) for his help with experiments and for fruitful discussion. The present research was financially supported by the Tanikawa Netsu-gijutsu Sinko Foundation (1997 Osaka).

*Author to whom correspondence should be addressed. Electronic address: naga-sho@oyna.cc.muroran-it.ac.jp

[1] *Ferro-Magnetic Materials*, edited by E. P. Wohlfarth, A Handbook on the Properties of Magnetically Ordered Substances Vol. 3 (North-Holland, Amsterdam, 1982), p. 603.

[2] F. K. Lotgering, Philips Res. Rep. **11**, 190 (1956).

[3] K. Miyatani, M. Ishikawa, and T. Tanaka, *Proceedings of the Sixth International Conference on Ferrites* (The Japan Society of Powder and Powder Metallurgy, Tokyo, 1992), p. 589.

[4] N. H. Van Maaren, G. M. Schaeffer, and F. K. Lotgering, Phys. Lett. **25A**, 238 (1967).

[5] M. Robbins, R. H. Willens, and R. C. Miller, Solid State Commun. **5**, 933 (1967).

[6] R. N. Shelton, D. C. Johnson, and H. Adrian, Solid State Commun. **20**, 1077 (1977).

[7] T. Hagino, Y. Seki, N. Wada, S. Tsuji, T. Shirane, K. Kumagai, and S. Nagata, Phys. Rev. B **51**, 12 673 (1995).

[8] T. Bitoh, T. Hagino, Y. Seki, S. Chikazawa, and S. Nagata, J. Phys. Soc. Jpn. **61**, 3011 (1992).

[9] G. W. Webb, Z. Fisk, J. J. Engelhardt, and S. D. Bader, Phys. Rev. B **15**, 2624 (1976).

[10] S. Nagata, T. Hagino, Y. Seki, and T. Bitoh, Physica B **194-196**, 1077 (1994).

[11] T. Furubayashi, T. Matsumoto, T. Hagino, and S. Nagata, J. Phys. Soc. Jpn. **63**, 3333 (1994).

[12] T. Hagino, Y. Seki, and S. Nagata, Physica C **235-240**, 1303 (1994).

[13] T. Hagino, T. Tojo, T. Atake, and S. Nagata, Philos. Mag. B **71**, 881 (1995).

[14] G. Oomi, T. Kagayama, I. Yoshida, T. Hagino, and S. Nagata, J. Magn. Magn. Mater. **140-144**, 157 (1995).

[15] J. Matsuno, T. Mizokawa, A. Fujimori, D. A. Zatsepin, V. R. Galakhov, E. Z. Kurmaev, Y. Kato, and S. Nagata, Phys. Rev. B **55**, R15 979 (1997).

[16] K. Kumagai, S. Tsuji, T. Hagino, and S. Nagata, in *Spectroscopy of Mott Insulators and Correlated Metals*, edited by A. Fujimori and Y. Tokura, Springer Series in Solid-State Sciences Vol. 119 (Springer-Verlag, Berlin, 1995), p. 255.

[17] K. Balcerek, Cz. Marucha, R. Wawryk, T. Tyc, N. Matsumoto, and S. Nagata, in *11th Seminar on Phase Transitions and Critical Phenomena, Wrocław and Polanica Zdrój, Poland, May, 1998*, edited by M. Kazimierski, Series in Physics and Chemistry of Solids (Institute of Low Temperature and Structure Reserch, Polish Academy of Sciences, Wrocław, 1998), p. 110.

[18] J. Tang, S. Uji, T. Terakura, T. Naka, T. Matsumoto, T. Furubayashi, A. Matsushita, S. Nagata, and N. Matsumoto (unpublished).

[19] T. Oda, M. Shirai, N. Suzuki, and K. Motizuki, J. Phys.: Condens. Matter **7**, 4433 (1995).

[20] T. Oda, M. Shirai, N. Suzuki, and K. Motizuki, Cryst. Res. Technol. **31**, 877 (1996).

[21] S. Nagata, N. Matsumoto, Y. Kato, T. Furubayashi, T. Matsumoto, J. P. Sanchez, and P. Vulliet, Phys. Rev. B **58**, 6844 (1998).

[22] E. Z. Kurmaev, V. R. Galakhov, D. A. Zatsepin, V. A. Trofimova, S. Stadler, D. L. Ederer, A. Moewes, M. M. Grush, T. A. Callcott, J. Matsuno, A. Fujimori, and S. Nagata, Solid State Commun. **108**, 235 (1998).

[23] S. Tsuji, K. Kumagai, N. Matsumoto, Y. Kato, and S. Nagata, Physica B **237-238**, 156 (1997).

[24] S. Tsuji, K. Kumagai, N. Matsumoto, and S. Nagata, Physica C **282-287**, 1107 (1997).

[25] E. König and G. König, in *Magnetic Properties of Coordination and Organometallic Transition Metal Compounds*, edited by K.-H. Hellwege and A. M. Hellwege, Landolt-Börnstein, New Series, Group II, Vol. 8 (Springer-Verlag, Berlin, 1976), p. 27.

[26] T. Furubayashi, T. Kosaka, J. Tang, T. Matsumoto, Y. Kato, and S. Nagata, J. Phys. Soc. Jpn. **66**, 1563 (1997).

[27] J. Tang, T. Matsumoto, T. Naka, T. Furubayashi, S. Nagata, and N. Matsumoto, Physica B **259-261**, 857 (1999).

[28] K. Koerts, Recl. Trav. Chim. Pays-Bas. **82**, 1099 (1963).

[29] H. Itoh, J. Phys. Soc. Jpn. **46**, 1127 (1979).

[30] N. Matsumoto, H. Honma, Y. Kato, S. Yasuzuka, K. Morie, N. Kijima, S. Ebisu, and S. Nagata, in *Proceedings of the 9thInternational Symposium on Superconductivity, Sapporo, Japan, 1996*, edited by S. Nakajima and M. Murakami [Adv. Supercond. **9**, 175 (1997)].

[31] T. Shirane, T. Hagino, Y. Seki, T. Bitoh, S. Chikazawa, and S. Nagata, J. Phys. Soc. Jpn. **62**, 374 (1993).

[32] E. Riedel, J. Pickardt, and J. Söchtig, Z. Anorg. Allg. Chem. **419**, 63 (1976).

[33] T. Kimoto (unpublished).

[34] L. F. Schneemeyer, J. K. Thomas, T. Siegrist, B. Batlogg, L. W. Rupp, R. L. Opila, R. J. Cava, and D. W. Murphy, Nature (London) **335**, 421 (1988).

[35] S. Chikazumi, in *Magnetism and Magnetic Materials*, edited by J. J. Becker, G. H. Lander, and J. J. Rhyne, AIP Conf. Proc. No. 29 (AIP, New York, 1976), p. 382.

[36] J. Q. Li, Y. Matsui, S. K. Park, and Y. Tokura, Phys. Rev. Lett. **79**, 297 (1997).